Ab initio studies of the tunneling magneto-Seebeck effect: Influence of magnetic material

Christian Heiliger,* Christian Franz, and Michael Czerner
I. Physikalisches Institut, Justus Liebig University, Giessen, Germany
(Received 22 March 2013; revised manuscript received 13 May 2013; published 13 June 2013)

We found a strong influence of the composition of the magnetic material on the temperature dependence of the tunneling magneto-Seebeck effect in MgO-based tunnel junctions. We use *ab initio* alloy theory to consider different Fe_xCo_{1-x} alloys for the ferromagnetic layer. Even a small change of the composition leads to strong changes in the magnitude or even in the sign of the tunneling magneto-Seebeck effect. This can explain differences between recent experimental results. In addition, changing the barrier thickness from six to ten monolayers of MgO leads to a nontrivial change of the temperature dependence. Our results emphasize that the tunneling magneto-Seebeck effect depends very crucially on and is very sensitive to material parameters and show that further experimental and theoretical investigations are necessary.

DOI: 10.1103/PhysRevB.87.224412 PACS number(s): 75.76.+j, 73.50.Jt, 73.63.−b, 85.30.Mn

I. INTRODUCTION

The recently theoretically predicted[1] and experimentally confirmed[2,3] tunneling magneto-Seebeck (TMS) effect in MgO-based tunnel junctions belongs to the new field of spin caloritronics.[4,5] In this field the spin-dependent charge transport is combined with energy or heat transport. This means that the spin degree of freedom is exploited in thermoelectrics.[6] Besides the TMS currently investigated effects in the field of spin caloritronics are the spin-Seebeck effect,[7,8] the magneto-Seebeck effect in metallic multilayers,[9] the thermal spin-transfer torque,[10] Seebeck spin tunneling,[11] thermally excited spin currents,[12] and the magneto-Peltier cooling.[13] In this paper we investigate the role of the ferromagnetic lead material on the TMS. We show that not only the temperature dependence but even the sign of the TMS effect depends crucially on the material composition.

The TMS effect is the change of the Seebeck coefficient with a change of the magnetic orientation of the ferromagnetic leads relative to each other in a tunnel junction. The size of the effect is given by the TMS ratio

$$\frac{S^P - S^{AP}}{\min(|S^P|,|S^{AP}|)}, \tag{1}$$

where S^P (S^{AP}) is the Seebeck coefficient for parallel (antiparallel) magnetic orientation of the ferromagnetic leads. Therefore the TMS effect is similar to the tunneling magnetoresistance effect (TMR),[14,15] where one considers the change of the electrical resistance with a change of the magnetic orientation. Note that in contrast to the resistance the Seebeck coefficient can be positive or negative. Hence the TMS ratio can have divergences whenever one of the Seebeck coefficients in Eq. (1) is zero.

II. METHOD

The tunnel junctions we study consist of a $Fe_xCo_{1-x}(001)/MgO/Fe_xCo_{1-x}(001)$ structure embedded between semi-infinite leads. These leads are just acting as reservoirs and are modeled by Cu in the bcc-Fe structure. For the Fe_xCo_{1-x} alloy we use a fixed lattice constant of 0.287 nm for all compositions. The thickness of both ferromagnetic leads is 20 monolayers, and only symmetric junctions are considered. For the MgO barrier we use six and ten monolayers. As in our previous studies[1,2] we use the ideal positions for the interface layers. In particular, no relaxation effects at the Fe_xCo_{1-x}/MgO interface are taken into account. That way, we really focus on the influence of the change of the electronic structure in the lead material by alloying. Although in most cases, e.g., by sputtering techniques, Fe_xCo_{1-x} is only stable in bcc structures for $x > 0.3$,[16] we consider the whole concentration range. Actually, with methods such as molecular beam epitaxy it is also possible to grow pure Co leads in a bcc structure.[17]

For the description of the Fe_xCo_{1-x} alloy we employ the coherent potential approximation (CPA)[18,19] recently implemented in our Korringa-Kohn-Rostoker (KKR) method.[20] Within the CPA the alloy is described by an effective medium, which is calculated self-consistently. For the description of the transport properties so-called vertex corrections are essential.[21–23] The CPA together with the vertex corrections leads, for FeCo alloys, basically to the same result as the supercell approach, where one has to average the transport properties over a larger number of different supercells.[20] In comparison to the supercell approach, the advantages of the CPA are a lower computational effort and the possibility to use an arbitrary composition. The transport coefficients, in particular, the transmission function $T(E)$, are calculated using the nonequilibrium Green's-function formalism implemented in the KKR method[24] including vertex corrections for the CPA.[20] From $T(E)$ we calculate the moments

$$L_n = \frac{2}{h}\int T(E)(E-\mu)^n[-d/dE f(E,\mu,\Theta)]dE, \tag{2}$$

where $f(E,\mu,\Theta)$ is the Fermi occupation function at a given energy E, electrochemical potential μ, and temperature Θ. In linear response the conductance G and the Seebeck coefficient S are given by[25]

$$G = e^2 L_0, \qquad S = -\frac{1}{e\Theta}\frac{L_1}{L_0}. \tag{3}$$

These quantities are calculated for parallel and antiparallel magnetic orientation of the Fe_xCo_{1-x} layers to eventually calculate the TMS ratio according to Eq. (1). Note that the conductance is basically the area under the transmission function times the derivative of the occupation function,

whereas the Seebeck coefficient is proportional to the expected value (or first moment) of the very same product. Therefore the Seebeck coefficient is determined by the asymmetry of the transmission function with respect to the Fermi level. Small modulations of the transmission function that have only a little influence on the area under that function may lead to strong changes of the geometric mean of the transmission function. For example, energetically, shifts of peaks in the transmission function due to a shift of the Fermi level can lead to a strong change of the geometric mean but at the same time to an almost unaffected area under the transmission function. Consequently, it can be expected that the Seebeck coefficient can depend crucially on changes of the transmission function, e.g., due to alloying of the magnetic material. All calculations are done in the atomic sphere approximation, and the cutoff for the angular momentum is 3. The k-point grids consist of 576 and 40 000 points in the whole Brillouin zone for the self-consistent and transport calculations, respectively.

III. RESULTS

One of our main results is shown in Fig. 1. There, the TMS ratio at room temperature for two different barrier thicknesses is given as a function of the Fe_xCo_{1-x} composition. It clearly shows that not only the magnitude but also the sign of the TMS ratio is very sensitive to the actual composition. This means that even small changes in the composition can drastically change the magnitude and even the sign of the TMS ratio. This could explain the small experimentally observed values[2,3] in comparison to the large values predicted for the pure materials[1] because in experiments compositions close to 50:50 Fe and Co are usually used. In addition, differences in the composition of the magnetic material can be a reason for the different signs observed in the experiments in Refs. 2 and 3.

Increasing the barrier thickness from six to ten monolayers can change the values significantly depending on the composition. In particular, the TMS ratio can increase as well as decrease with increasing barrier thickness, and even the sign can change. To analyze the TMS further the bottom viewgraph of Fig. 1 shows the Seebeck coefficients at room temperature for parallel and antiparallel magnetic configurations that lead to the discussed TMS ratios according to Eq. (1). Likewise, here, no general trend is visible, and the Seebeck coefficient can be decreased or increased by increasing the barrier thickness.

Up to now we have discussed the TMS only at room temperature. In Fig. 2 we show for the different compositions considered the temperature dependence of the TMS ratio for six and ten monolayers of MgO. Note that the temperature enters the calculation only in the occupation function in Eq. (2). The temperature dependencies for the pure materials were already discussed in Ref. 1. Figure 2 shows that the temperature dependence is rather involved and that there is also no clear trend visible when the composition is changed. We illustrate this with two examples. First, in the bottom left panel all shown compositions have a moderate increase except for the $Fe_{0.5}Co_{0.5}$ alloy, which has a TMS ratio strongly increasing with temperature. Second, in the bottom right panel for $Fe_{0.7}Co_{0.3}$ and $Fe_{0.9}Co_{0.1}$ the TMS ratio is decreasing with increasing temperature, but for the composition in between, e.g., $Fe_{0.8}Co_{0.2}$, the TMS ratio is increasing. Besides the

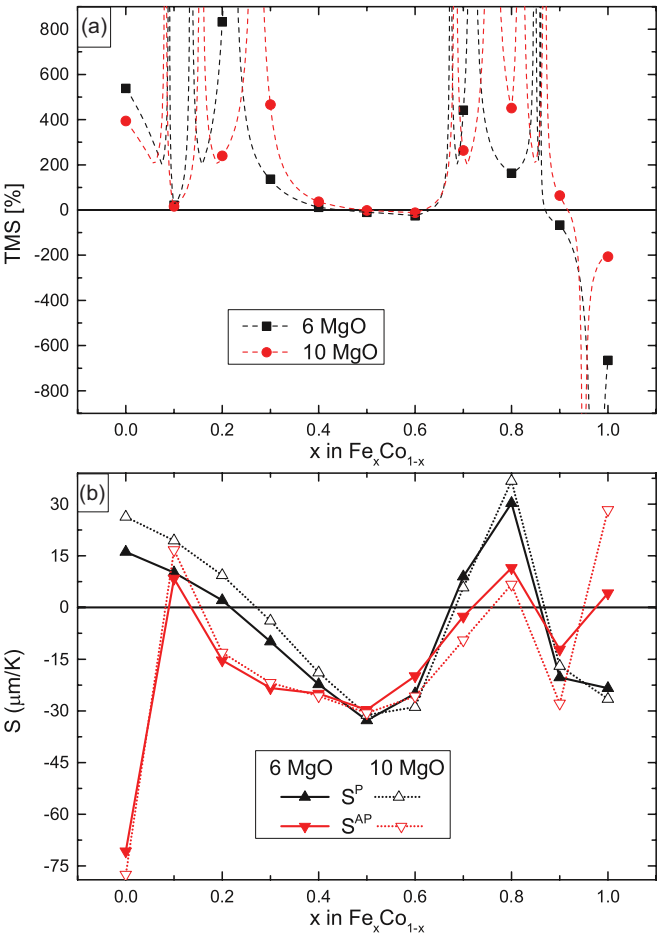

FIG. 1. (Color online) (a) TMS ratio as a function of Fe_xCo_{1-x} composition at room temperature for two different barrier thicknesses. (b) Seebeck coefficient for parallel, S^P, and antiparallel, S^{AP}, magnetic configurations of the ferromagnetic layers as a function of the Fe_xCo_{1-x} composition at room temperature for two different barrier thicknesses. Note that the connecting lines are just a guide to the eyes. In (b) a linear interpolation between the sampling points is used. These interpolated lines are used to calculate the connecting lines in (a) according to Eq. (1). In particular, each time one of the Seebeck coefficients is zero, the TMS ratio has a divergence.

dependence on the composition the change in the barrier thickness can also lead to quite different temperature dependencies, for example, those visible for $Fe_{0.2}Co_{0.8}$, $Fe_{0.5}Co_{0.5}$, and $Fe_{0.8}Co_{0.2}$.

Features of the temperature dependence of the TMS ratio are divergences, which occur when one of the Seebeck coefficients goes through zero. Except for pure Fe a divergence is observed only for the $Fe_{0.1}Co_{0.9}$ alloy. Another interesting feature is a sign change of the TMS ratio with temperature, which is also observed experimentally.[2] To get an overview of when the sign changes occur we compile in Table I the temperatures at which the sign changes occur and in which direction it proceeds. For the compositions where no sign change occurs we give the corresponding sign of the TMS ratio over the whole temperature range. We see that there is a sign change of the TMS ratio only for certain compositions and that it also depends on the barrier thickness. Moreover, a comparison of $Fe_{0.6}Co_{0.4}$ and $Fe_{0.7}Co_{0.3}$ shows again that the

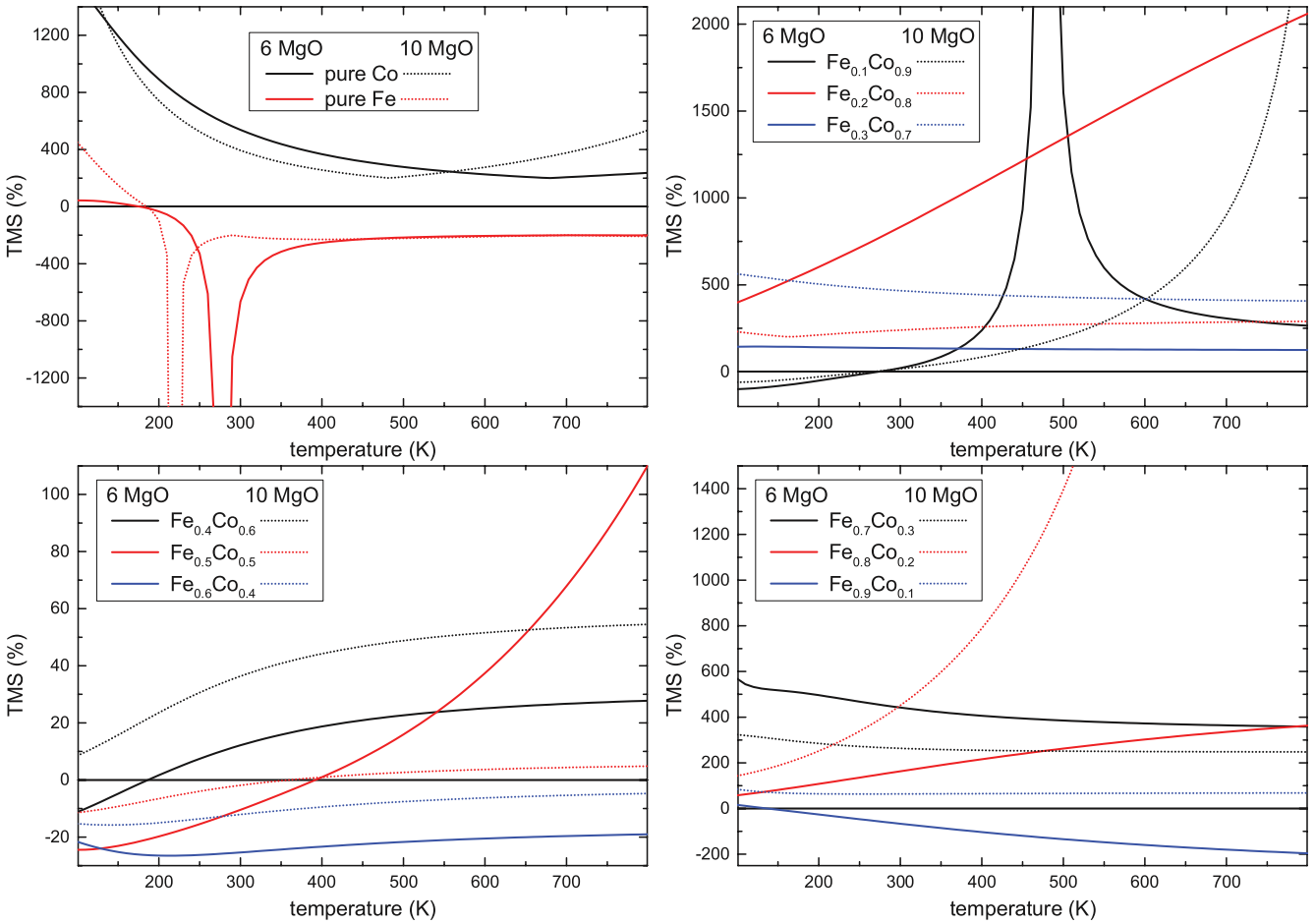

FIG. 2. (Color online) TMS ratio as a function of temperature for pure Fe and Co (as already published in Ref. 1) and for different alloy compositions of Fe_xCo_{1-x}. For the barrier we use six and ten monolayers of MgO.

sign of the TMS ratio crucially depends on the composition of the ferromagnetic material.

For completeness, we give in Fig. 3 the corresponding temperature dependencies of the Seebeck coefficients for parallel and antiparallel magnetic configurations, which lead to the temperature dependencies of the TMS shown in Fig. 2. It shows that a vanishing Seebeck coefficient in the antiparallel configuration is responsible for all the observed divergences, which is just by accident and has no physical reason.

Up to now, all the presented results seem unsystematic with respect to the alloy composition. The underlying physical quantity is the transmission function $T(E)$, which determines the transport properties according to Eqs. (2) and (3). Consequently, in Fig. 4 we look at $T(E)$ for the parallel and antiparallel configuration for the two considered barrier thicknesses. For the transmission in the parallel configuration [Figs. 4(a) and 4(c)] a systematic and continuous change with the ferromagnetic layer composition is visible. For example, for six monolayers of MgO there is a peak in $T^P(E)$ below the Fermi level, which moves continuously to higher energies with increasing Fe concentration. For an Fe concentration of about 70% a second peak occurs at energies below the Fermi level. One has to keep in mind that the Seebeck coefficient is proportional to the first moment of the transmission function

TABLE I. Temperatures of the sign changes T_{sc} of the TMS ratio, if present, extracted from the different temperature dependencies given in Fig. 2. In addition, the direction of the sign change is given: $n \to p$ ($p \to n$) means a change from negative to positive (positive to negative) with increasing temperature. If no sign change is present, n or p gives the sign of the TMS ratio over the whole temperature range.

		x in Fe_xCo_{1-x}										
		0.0	0.1	0.2	0.3	0.4	0.5	0.6	0.7	0.8	0.9	1.0
Six MgO monolayers	T_{sc} (K)		285			185	390				140	175
		p	$n \to p$	p	p	$n \to p$	$n \to p$	n	p	p	$p \to n$	$p \to n$
Ten MgO monolayers	T_{sc} (K)		265				360					185
		p	$n \to p$	p	p	p	$n \to p$	n	p	p	p	$p \to n$

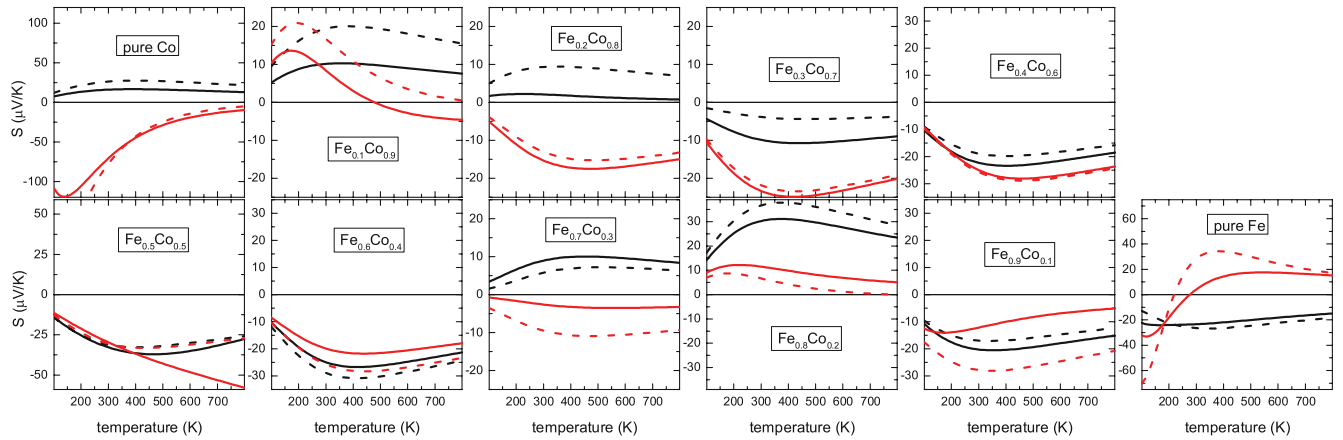

FIG. 3. (Color online) Seebeck coefficients for parallel (black) and antiparallel (red) magnetic configurations for different Fe_xCo_{1-x} compositions. For the barrier we use six (solid lines) and ten (dashed lines) monolayers of MgO.

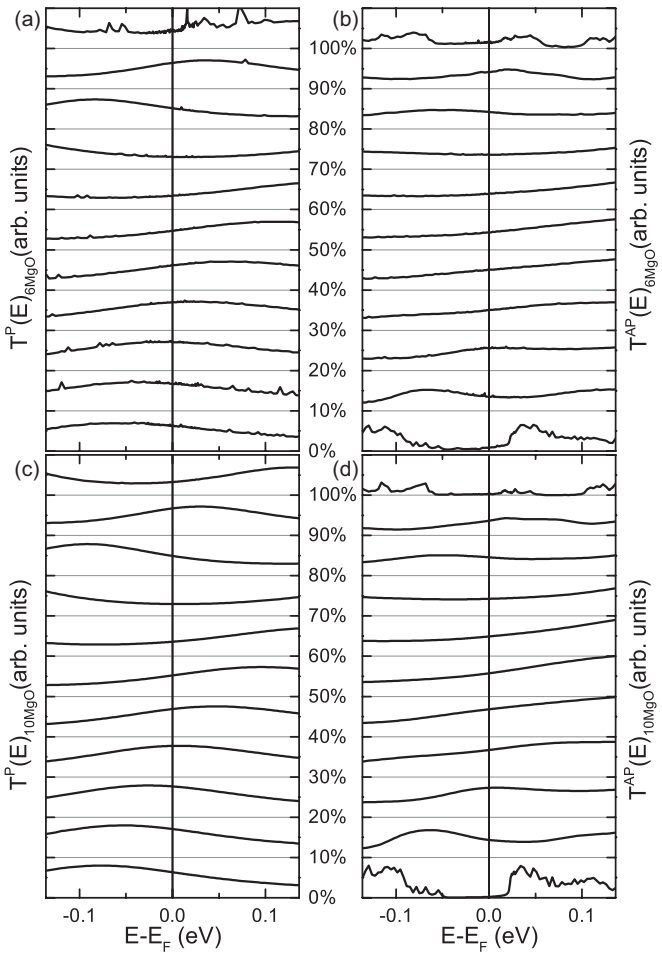

FIG. 4. Transmission function $T(E)$ for (a) the parallel configuration and six monolayers of MgO, (b) the antiparallel configuration and six monolayers of MgO, (c) the parallel configuration and ten monolayers of MgO, and (d) the antiparallel configuration and ten monolayers of MgO for different Fe contents in Fe_xCo_{1-x}. Note that within each of the four panels the same scale of T is used. The scale of T^{AP} is 0.05 (0.03) times the corresponding scale of T^P for six (ten) monolayers of MgO, and the scale of T^P for ten monolayers of MgO is 0.0015 times the scale of T^P for six monolayers of MgO.

times the derivative of the occupation function [see Eqs. (2) and (3)]. Consequently, only the asymmetry of $T(E)$ is important, and this is changed by the discussed movement of peaks. With this the given temperature dependencies of S^P in Fig. 3 can be understood. Moreover, due to the continuous change of $T^P(E)$ one can interpolate to other compositions without doing a full *ab initio* calculation.

The reason for this continuous change in the parallel configuration can be explained with the band structure. First, it is important to realize that the transport is dominated by the majority spin in Fe and Co where a Δ_1 band is present and dominates the transport.[26–28] By alloying, this band is only weakly affected, and the composition primarily shifts the position of the Fermi level. And this shift of the Fermi level corresponds to the shift of the transmission function with the composition.

However, this is no longer the case for the antiparallel configuration. Here, the simple Δ_1 band does not contribute to the transport, and the transport is dominated by pockets within the Brillouin zone.[26] This is clearly visible in the rich structure of T^{AP} for the pure materials. In the alloy case the band structure is broadened by disorder scattering, leading to a "washed out" transmission function. Going through the different compositions, no clear continuous change is visible, in particular, close to the pure materials. Therefore the rather involved temperature dependencies of the TMS ratio can be traced back to the complicated change with composition of the transmission function in the antiparallel magnetic configuration.

IV. CONCLUSION

In conclusion, we show that the TMS ratio is crucially dependent on the alloy composition of the magnetic material. The behavior seems unsystematic but can be traced back to a simple concentration dependence of the parallel transmission and a complicated change of the transmission function in the antiparallel magnetic configuration. This leads to a strong dependence not only of the magnitude but also of the sign of the TMS ratio even for small changes in compositions. In general, the TMS ratios are smaller for compositions close to a 50:50 split in comparison to compositions closer to the

pure materials. Moreover, small changes in compositions can cause the different signs of the TMS which were observed in experiments.[2,3] To achieve a full understanding of the TMS in the MgO-based tunnel junctions further experimental and theoretical studies are necessary.

ACKNOWLEDGMENTS

We thank M. Münzenberg and M. Walter for useful discussions and acknowledge support from DFG SPP 1386 and DFG Grant No. HE 5922/1-1.

*christian.heiliger@physik.uni-giessen.de

[1] M. Czerner, M. Bachmann, and C. Heiliger, Phys. Rev. B **83**, 132405 (2011).
[2] M. Walter, J. Walowski, V. Zbarsky, M. Münzenberg, M. Schäfers, D. Ebke, G. Reiss, A. Thomas, P. Peretzki, M. Seibt, J. S. Moodera, M. Czerner, M. Bachmann, and C. Heiliger, Nat. Mater. **10**, 742 (2011).
[3] N. Liebing, S. Serrano-Guisan, K. Rott, G. Reiss, J. Langer, B. Ocker, and H. W. Schumacher, Phys. Rev. Lett. **107**, 177201 (2011).
[4] G. E. W. Bauer, A. H. MacDonald, and S. Maekawac, Solid State Commun. **150**, 459 (2010).
[5] G. E. W. Bauer, E. Saitoh, and B. J. van Wees, Nat. Mater. **11**, 391 (2012).
[6] M. Johnson and R. H. Silsbee, Phys. Rev. B **35**, 4959 (1987).
[7] K. Uchida, S. Takahashi, K. Harii, J. Ieda, W. Koshibae, K. Ando, S. Maekawa, and E. Saitoh, Nature (London) **455**, 778 (2008).
[8] J. Xiao, G. E. W. Bauer, K. Uchida, E. Saitoh, and S. Maekawa, Phys. Rev. B **81**, 214418 (2010).
[9] L. Gravier, S. Serrano-Guisan, F. Reuse, and J. P. Ansermet, Phys. Rev. B **73**, 024419 (2006).
[10] X.-T. Jia, K. Xia, and G. E. W. Bauer, Phys. Rev. Lett. **107**, 176603 (2011).
[11] J. C. Le Breton, S. Sharma, H. Saito, S. Yuasa, and R. Jansen, Nature (London) **475**, 82 (2011).
[12] O. Tsyplyatyev, O. Kashuba, and V. I. Fal'ko, Phys. Rev. B **74**, 132403 (2006).
[13] M. Hatami, G. E. W. Bauer, Q. F. Zhang, and P. J. Kelly, Phys. Rev. B **79**, 174426 (2009).
[14] J. S. Moodera, L. R. Kinder, T. M. Wong, and R. Meservey, Phys. Rev. Lett. **74**, 3273 (1995).
[15] T. Miyazaki and N. Tezuka, J. Magn. Magn. Mater. **139**, L231 (1995).
[16] F. Bonell, T. Hauet, S. Andrieu, F. Bertran, P. Le Fevre, L. Calmels, A. Tejeda, F. Montaigne, B. Warot-Fonrose, B. Belhadji, A. Nicolaou, and A. Taleb-Ibrahimi, Phys. Rev. Lett. **108**, 176602 (2012).
[17] S. Yuasa, A. Fukushima, H. Kubota, Y. Suzuki, and K. Ando, Appl. Phys. Lett. **89**, 042505 (2006).
[18] W. H. Butler, Phys. Rev. B **31**, 3260 (1985).
[19] J. Zabloudil, R. Hammerling, L. Szunyogh, and P. Weinberger, *Electron Scattering in Solid Matter: A Theoretical and Computational Treatise*, Springer Series in Solid-State Sciences Vol. 147 (Springer, Berlin, 2005).
[20] C. Franz, M. Czerner, and C. Heiliger, arXiv:1305.2399.
[21] B. Velický, Phys. Rev. **184**, 614 (1969).
[22] K. Carva, I. Turek, J. Kudrnovský, and O. Bengone, Phys. Rev. B **73**, 144421 (2006).
[23] Y. Ke, K. Xia, and H. Guo, Phys. Rev. Lett. **100**, 166805 (2008).
[24] C. Heiliger, M. Czerner, B. Yu. Yavorsky, I. Mertig, and M. D. Stiles, J. Appl. Phys. **103**, 07A709 (2008).
[25] Y. Ouyang and J. Guo, Appl. Phys. Lett. **94**, 263107 (2009).
[26] W. H. Butler, X.-G. Zhang, T. C. Schulthess, and J. M. MacLaren, Phys. Rev. B **63**, 054416 (2001).
[27] C. Heiliger, P. Zahn, and I. Mertig, Mater. Today **9**, 46 (2006).
[28] C. Heiliger, P. Zahn, B. Yu. Yavorsky, and I. Mertig, Phys. Rev. B **77**, 224407 (2008).